



Electrical and magnetic properties of ZnNiO thin films deposited by pulse laser deposition*

Jie JIANG, Xue-tao WANG, Li-ping ZHU^{†‡}, Li-qiang ZHANG, Zhi-guo YANG, Zhi-zhen YE

(State Key Laboratory of Silicon Materials, Department of Materials Science and Engineering,
 Zhejiang University, Hangzhou 310027, China)

[†]E-mail: zlp1@zju.edu.cn

Received Dec. 31, 2010; Revision accepted Feb. 27, 2011; Crosschecked June 21, 2011

Abstract: ZnNiO thin films with different contents of Ni (0–10 at.%) were fabricated on quartz and Si (100) substrates by pulsed laser deposition (PLD). We measured the samples by X-ray diffraction (XRD), field-emission scanning electron microscope (FE-SEM), X-ray photoelectron spectroscopy (XPS), ultraviolet-visible spectrometer (UV-VIS), and Hall testing. When the Ni contents were below 3 at.%, partial Zn²⁺ ions were replaced by the Ni²⁺ ions without forming any other phases, which enhanced the conductivity of the film. When the Ni contents were above 3 at.%, Ni ions were at the interstitial sites, and Ni-related clusters and defects were able to emerge in the films, resulting in a worsening of electrical and optical properties. A ferromagnetic hysteresis with a coercive force of approximately 30 Oe was observed in the ZnNiO film with a Ni content of 3 at.% at room temperature.

Key words: ZnNiO thin films, Electric property, Ferromagnetic, Transmittance, Pulsed laser deposition (PLD)

doi: 10.1631/jzus.A1000525

Document code: A

CLC number: O472+.5

1 Introduction

ZnO is a compound semiconductor with a wide direct band gap of 3.37 eV and a large excitation binding energy of 60 meV at room temperature, and a promising candidate for electrical and optoelectronic devices (Tang *et al.*, 1998; Look, 2001). ZnO is an intrinsic n-type material, the electrical and optical properties of which can be tuned by doping with typical donor doping elements such as Ga, Al, In, and H (Yamada *et al.*, 2007; Li *et al.*, 2008; Peng *et al.*, 2008), and acceptor doping elements such as N (Huang *et al.*, 2002; Fang *et al.*, 2007), P (Kim *et al.*, 2008) and Li (Zeng *et al.*, 2006), and Na (Lin *et al.*, 2008; 2009). In addition, there are other special

doping elements such as Mn (Wang *et al.*, 2004), Co (Dorneles *et al.*, 2007), Fe (Parra-Palomino *et al.*, 2008), and Ni (Mitra *et al.*, 2006), with magnetic properties, forming dilute magnetic semiconductors (DMSs). Realization of ferromagnetic behavior in wide band gap materials provides an important insight into spin injection applications such as those in spin filters and spin transport media (Pan *et al.*, 2008). ZnO-based DMSs have received considerable attention in recent years due to their outstanding optical and electrical properties (Liu *et al.*, 2006).

Thus far, relatively few studies have focused on the ZnNiO system, since its preparation is particularly challenging due to the large driving force for phase segregation into NiO and ZnO (Jayaram and Rani, 2001). Mitra *et al.* (2006) have reported that the electric conductivity of Ni doped ZnO films increased as the concentration of Ni increased, while Wakano *et al.* (2001) found the opposite. The resistivity of Ni doped ZnO film changed from 10¹⁷ cm⁻³ (high resistivity) to 10⁻³ cm⁻³ (low resistivity), and is affected by prepara-

[‡] Corresponding author

* Project supported by the National Natural Science Foundation of China (No. 51072181), and the Doctoral Fund of Ministry of Education of China (No. 20090101110044)

© Zhejiang University and Springer-Verlag Berlin Heidelberg 2011

tion and procedure parameters. ZnNiO film is considered to be a promising DMS that can achieve room temperature ferromagnetism. Sato and Katayama-Yoshida (2001) believed that the ferromagnetic state could be, theoretically, stabilized by electron doping. As a result, the electrical property is an important influencing factor on the magnetism of ZnNiO films. In this paper, we fabricated the ZnO and ZnNiO films DMS by pulsed laser deposition (PLD) and studied the influence of Ni contents on the structural, electrical, optical, and magnetic properties of ZnNiO films.

2 Experimental

ZnO and ZnNiO thin films were deposited on quartz and Si (100) substrates by PLD. The substrates were cleaned by acetone before the deposition. The ceramic targets were prepared by mixing ZnO (99.99%) and Ni (99.99%) powders in proportion. A KrF excimer laser (Compex102, Lambda physic, Germany) was used as the ablation source. The laser power was 280 mJ, the repetition frequency was 5 Hz, the working pressure in the chamber was 0.02 Pa with O₂ as the ambient gas, and the substrates were held at 500 °C during the film deposition.

The morphologies of the films were observed by field-emission scanning electron microscope (FE-SEM) (S-4800, Hitachi, Japan). The crystallographic structure of the films was investigated by the Bede D1 X-ray diffraction (XRD) (Bede, U.K) system with Cu K α radiation ($\lambda=0.15406$ nm). The electrical properties were investigated by using a four-point probe van der Pauw configuration (HL5500PC) at room temperature. The absorption spectra of the films were measured at room temperature on an ultraviolet-visible (UV-VIS) spectrometer (UV3600, Shimadzu, Japan). The magnetic properties were measured by a superconducting quantum interference device (SQUID) MPMS-XL magnetometer of Quantum Design Company (USA), and the measurement accuracy is up to 10⁻⁸ emu.

3 Results and discussion

Fig. 1 shows the typical FE-SEM images of the ZnNiO thin films with different Ni contents. All the films have a nearly smooth surface and uniform grain

size. The composition analysis of the ZnNiO films by the energy dispersive X-ray spectroscopy (EDS) shows that Ni contents are 0.8 at.%, 2.7 at.%, 4.5 at.%, and 9.8 at.% in the thin films corresponding to 1 at.%, 3 at.%, 5 at.%, and 10 at.%, respectively, in the Ni doped ZnO ceramic targets. The thickness of all the ZnNiO thin films were about 400 nm, which were measured in the cross section SEM image (not shown here).

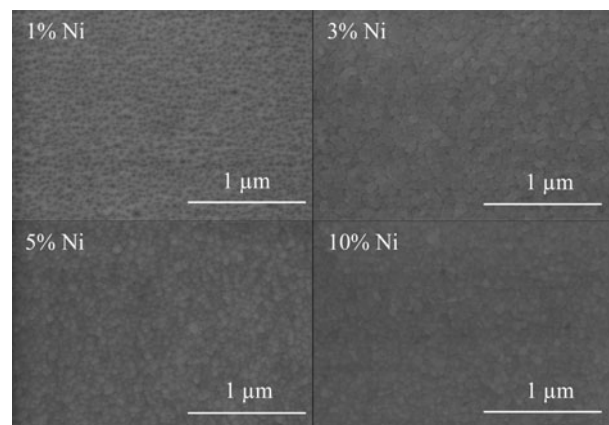


Fig. 1 Scanning electron microscope images of the ZnNiO films with different Ni contents: 1 at.% (a), 3 at.% (b), 5 at.% (c), and 10 at.% (d)

Fig. 2a shows the XRD patterns of ZnNiO samples with different Ni contents and that of pure ZnO thin film for comparison. It can be seen that only one (002) orientation peak around 34° is observed in all the samples, which reveals that all the thin films growing along c-axis of ZnO perpendicular to substrate have a high quality and Ni dopant cannot change the structure of ZnO. Fig. 2b shows the (002) peaks of the XRD patterns of the ZnNiO films with different Ni contents, in which the intensity is normalized for better comparison. Theoretically, since the ion radius of Ni²⁺ (0.69 Å) is smaller than that of Zn²⁺ (0.74 Å), with the assumption that all the dopant Ni would substitute for Zn, the (002) peak of the ZnNiO film should move to larger angles when compared to that of pure ZnO film ($2\theta=34.46^\circ$, where θ is the half diffraction angle) obtained at the same condition. And it is obvious that the peak indeed moves to a larger angle for the film with 1 at.% doping. However, for the film with 5 at.% Ni doping content, the peak shifts to a smaller angle. We believe that some of the incorporated Ni ions might lie at the

interstitial sites, leading to a lattice expansion. As the Ni contents increase, the Ni ions at the crystal lattices and interstitial sites may reach saturation, the peak thereby remaining at the same angle. The Ni-related clusters and defects, such as NiO, might be formed by the superfluous Ni dopant in the ZnNiO films with a large content of Ni. The grain size is calculated by Scherer's equation: $D=0.89\lambda/\beta\cos\theta$, where D denotes the diameter along c -axis, λ is the wavelength of X-ray ($\lambda=0.15406$ nm), and β is the full width at half maximum (FWHM). By calculation, we obtain the results that the films have the grain size of 32.63, 32.12, 31.56, 28.69, and 28.95 nm, respectively. This indicates that the crystal quality lessened as the Ni content increased.

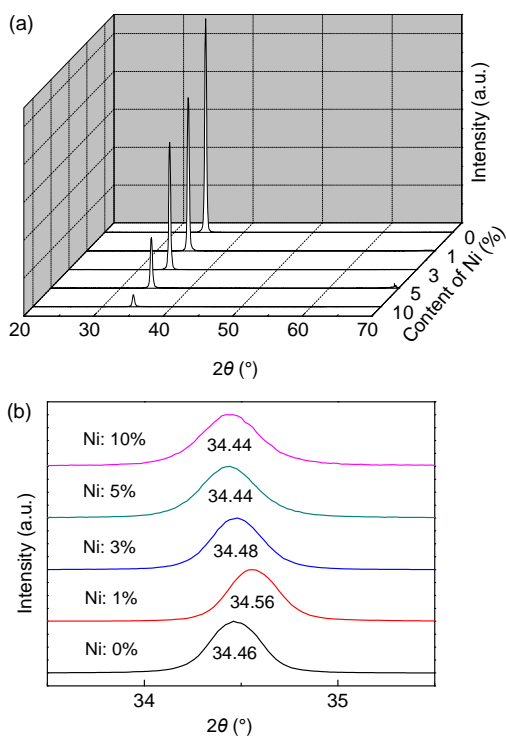


Fig. 2 (a) X-ray diffraction (XRD) patterns of the ZnNiO films with different Ni contents; (b) (002) peaks of XRD patterns of the ZnNiO films

The chemical states of the elements present are discussed according to the X-ray photoelectron spectroscopy (XPS) measurements. The substitution of Ni ions was confirmed by Ni 2p XPS spectrum (Fig. 3). The graphs of the ZnNiO films with different Ni contents were shifted for comparison and the binding energies were corrected for the charging effect, with

reference to the C 1s line at 284.8 eV. The Ni 2p_{3/2} peak occurs at (855.5±0.1) eV, while Ni 2p_{1/2} peak locates at (873.0±0.1) eV. Corresponding satellite structures were clearly observed at (860.5±0.5) and (880.0±0.5) eV, respectively. The Ni 2p_{3/2} peak position was close to that of NiO, but quite different from those of Ni and Ni₂O₃, which indicates that Ni ions in ZnO films might have a valence of +2 (Wagner *et al.*, 1979; Yu *et al.*, 2001). The energy difference between the Ni 2p_{3/2} and 2p_{1/2} peaks is about 17.5 eV, which is strikingly different from that of NiO (18.4 eV) (Wagner *et al.*, 1979). The above results strongly suggested that Ni atoms were successfully incorporated into ZnO. We also did not find any NiO clusters and defects in the ZnNiO films with a high content of Ni and believed that the content of Ni-related clusters and defects might be so small that they were not measurable by XPS.

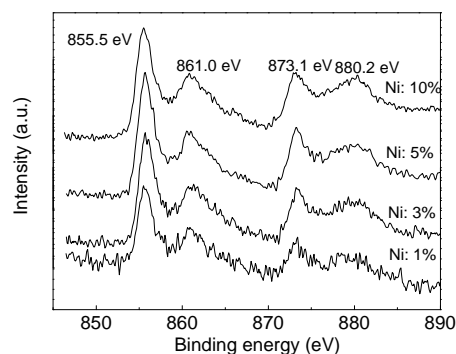


Fig. 3 X-ray photoelectron spectra of Ni in the ZnNiO films

Fig. 4 shows the O 1s XPS spectrum. The asymmetry and stretching of the absorption peak indicates different chemical states of the O element. The absorption peak of O 1s can be divided into two nearly Gaussian peaks, which are centered at (530.0±0.3) and (531.5±0.3) eV. The peak on the low binding energy side at 530.0 eV is attributed to O²⁻ ions on the wurtzite structure of the hexagonal Zn²⁺ ion array, surrounded by Zn (or substitution Ni) atoms (Chen *et al.*, 2000). The high binding-energy peak centered at 531.5 eV is associated with O²⁻ ions that are in oxygen-deficient regions within the matrix of ZnO (Futsuhara *et al.*, 1998; Li *et al.*, 2009). As the Ni contents increases, the peak at about 530 eV first moves to high binding energy and then back to low binding energy. It is indicated that the oxidation state of the O ion in the crystal lattice of the ZnNiO film is

the lowest with the Ni content of 3 at.% because of the highest binding energy. And the peaks at about 531.5 eV show blueshift as a whole, which reveals that the oxidation state of the O ion in oxygen-deficient regions is more stable. Therefore, more defects will be formed and the crystal quality will be worse as the Ni contents increase, which agrees with the XRD analysis.

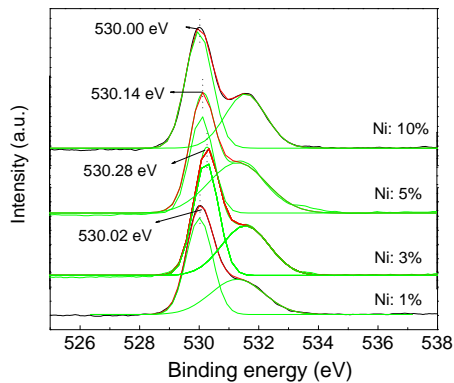


Fig. 4 X-ray photoelectron spectra of O in the ZnNiO films

Fig. 5 gives the transmission spectra of the ZnO and ZnNiO films. As the Ni content increases, the transmission rate of the films decrease and the band edge shows red shift when the Ni content reaches 10 at.%. The variation of the band edge is similar to results from other research group (Yu *et al.*, 2008). The band gap of the films for the Ni contents of 1 at.%, 3 at.%, and 5 at.% is 3.28 eV, while for the Ni content of 10 at.% is 3.19 eV by calculation (not shown here). This is because the band gap may be reduced by the tensile stress and defects caused by the Ni ions at the interstitial sites or the Ni-related

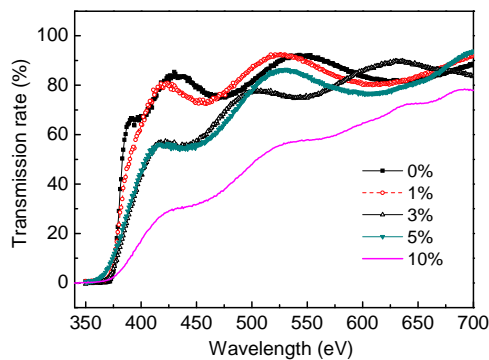


Fig. 5 Transmission spectra of the ZnNiO films with different Ni contents

clusters in the ZnNiO films with large content of Ni. The Ni dopant can weaken the optical property of ZnO film and change the band gap energy. However, the mechanisms behind the decrease in band gap energy with Ni doping are still unclear and need further study.

The Hall measurements demonstrate that the ZnNiO thin films are n-type semiconductor. Fig. 6 shows the changes of the resistivity, electron mobility, and carrier concentration in the ZnNiO films as the Ni contents increased. The resistivity of the pure ZnO film is 0.023 $\Omega\cdot\text{cm}$, which decreased a little on light doping (1 at.% and 3 at.%) and significantly increased on heavy doping (5 at.% and 10 at.%). Burstein (1954) found that the Fermi level (E_F) of Fe, Co, and Ni doped ZnO located near the top of valence band and the partial density of states of Fe, Co, and Ni near the E_F were large. Mitra *et al.* (2006) pointed out that the d states of Ni near E_F would split to a lower doublet e_g state and a higher energy triplet t_{2g} state. The t_{2g} further splits into bonding and antibonding states after coupling with the p orbits of the valence band. The antibonding state has higher energy and contains itinerant electrons. The energy of the antibonding state lies close to the bottom of the conduction band and the itinerant electrons are likely to jump to the conduction band, which enhances the conductivity. This can be clearly confirmed by the behavior of the resistivity of the ZnNiO films on light doping in our work. Due to the replacement of Zn^{2+} for Ni^{2+} the itinerant electron concentration increases with the Ni contents when the Ni contents are below 3 at.%, resulting in lowering of the resistivity. This is contradictory to heavy doping because of the worsening of crystal quality. From earlier studies, we know that the

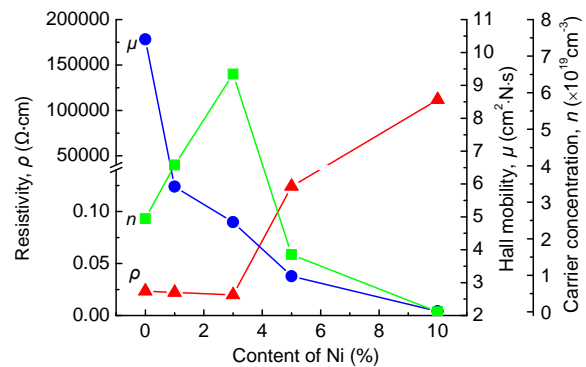


Fig. 6 Influence of Ni contents on the resistivity, electron mobility, and carrier concentration of the ZnNiO films

intrinsic defects are mainly native H, which cause the n-type electric conductivity in the pure ZnO film (McCluskey and Jokela, 2009). The electron concentration of the pure ZnO film in our study is $2.5 \times 10^{19} \text{ cm}^{-3}$, which is slightly enhanced by the Ni doping when the Ni contents are below 3 at.%. This might be the reason that the Ni ions at the interstitial sites provide electrons and increase the electron concentration. When the Ni contents are above 5 at.%, the electron concentration decreases because of the Ni-related clusters and defects that provide many holes. For the Hall mobility, the main factors of the influence are ion scattering and lattice scattering. As the Ni content increases, ion scattering and lattice scattering strengthen after the Ni-related clusters and defects emerge, such that the Hall mobility decreases.

The magnetic measurements of ZnNiO films with different Ni contents have been performed at room temperature. Fig. 7 presents the magnetization hysteresis (magnetization-field, M - H) loop for the ZnNiO films with 3 at.% Ni doping at different applied magnetic fields, and the inset of Fig. 7 is the enlarged partial view. It can be seen that the film with 3 at.% Ni doping exhibits distinct ferromagnetic hysteresis with the coercive force of approximately 30 Oe and saturation magnetization of 0.12 emu/g (about $0.06 \mu_{\text{B}}/\text{atom}$) at room temperature. Liu *et al.* (2008) have reported saturation magnetization of $0.02 \mu_{\text{B}}/\text{atom}$ as-deposited and $0.06 \mu_{\text{B}}/\text{atom}$ Ar-annealed, which is similar to our results. For the films with Ni contents above and below 3 at.%, we did not find any ferromagnetism. We believe that the observed ferromagnetism is the intrinsic property of the ZnNiO films, because we did not detect any Ni cluster or NiO in XRD and XPS measurements. The origin of room temperature ferromagnetism observed in ZnNiO

system remains a controversial subject (Liu *et al.*, 2009). From Fig. 6, we see that the carrier concentration is the highest and the resistivity is the lowest for the films with 3 at.% Ni doping. Therefore, the positive magnetization behavior might be affected by electrical properties (Wakano *et al.*, 2001). Considering the long-range interaction properties of ferromagnetic spin-spin coupling, the magnetic characteristics of the ZnNiO films are mostly related to Ni incorporating content and their microstructure (Yu *et al.*, 2008).

4 Conclusions

Different Ni concentrations of the ZnNiO thin films were prepared by PLD. By Ni doping, the electrical and optical properties were changed and the ferromagnetism emerged. In our experimental conditions, the solubility of Ni is about 3 at.%. When the Ni contents are below 3 at.%, the resistivity decreases a little, while the carrier concentration increases. When the Ni contents are above 3 at.%, the transmission rate and the carrier concentration decrease rapidly and the resistivity increases remarkably, which might be due to the formation of Ni-related clusters and defects. Also, a ferromagnetic hysteresis with the coercive force of approximately 30 Oe was measured for the ZnNiO film with the Ni content of 3 at.% at room temperature, which might be affected by the electrical properties.

References

- Burstein, E., 1954. Anomalous optical absorption limit in InSb. *Physical Review*, **93**(3):632-633. [doi:10.1103/PhysRev.93.632]
- Chen, M., Wang, X., Yu, Y.H., Pei, Z.L., Bai, X.D., Sun, C., Huang, R.F., Wen, L.S., 2000. X-ray photoelectron spectroscopy and auger electron spectroscopy studies of Al-doped ZnO films. *Applied Surface Science*, **158**(1-2): 134-140. [doi:10.1016/S0169-4332(99)00601-7]
- Dorneles, L.S., Venkatesan, M., Gunning, R., Stamenov, P., Alaria, J., Rooney, M., Lunney, J.G., Coey, J.M.D., 2007. Magnetic and structural properties of Co-doped ZnO thin films. *Journal of Magnetism and Magnetic Materials*, **310**(2):2087-2088. [doi:10.1016/j.jmmm.2006.10.1017]
- Fang, Z.Q., Claflin, B., Look, D.C., Kerr, L.L., Li, X.N., 2007. Electron and hole traps in N-doped ZnO grown on p-type Si by metalorganic chemical vapor deposition. *Journal of Applied Physics*, **102**(2):023714. [doi:10.1063/1.2759181]
- Futsuhara, M., Yoshioka, K., Takai, O., 1998. Optical

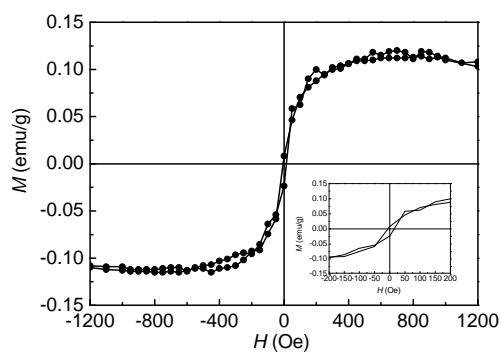


Fig. 7 Magnetization hysteresis (M - H) loop for the ZnNiO films with 3 at.% Ni content

- properties of zinc oxynitride thin films. *Thin Solid Films*, **317**(1-2):322-325. [doi:10.1016/S0040-6090(97)00646-9]
- Huang, J.Y., Ye, Z.Z., Chen, H.H., Zhao, B.H., Wang, L., 2002. Growth of N-doped p-type ZnO films using ammonia as dopant source gas. *Journal of Material Science Letters*, **22**(4):249-251. [doi:10.1023/A:1022347910122]
- Jayaram, V., Rani, B.S., 2001. Soft chemical routes to the synthesis of extended solid solutions of wurtzite ZnO-MO (M=Mg, Co, Ni). *Materials Science Engineering A*, **304-306**:800-804. [doi:10.1016/S0921-5093(00)01575-6]
- Kim, H.S., Lugo, F., Pearton, S.J., Norton, D.P., Wang, Y.L., Ren, F., 2008. Phosphorus doped ZnO light emitting diodes fabricated via pulsed laser deposition. *Applied Physics Letters*, **92**(11):112108. [doi:10.1063/1.2900711]
- Li, Q.H., Zhu, D.L., Liu, W.J., Liu, Y., Ma, X.C., 2008. Optical properties of Al-doped ZnO thin films by ellipsometry. *Applied Surface Science*, **254**(10):2922-2926. [doi:10.1016/j.apsusc.2007.09.104]
- Li, L., Fang, L., Zhou, X.J., Liu, Z.Y., Zhao, L., Jiang, S., 2009. X-ray photoelectron spectroscopy study and thermoelectric properties of Al-doped ZnO thin films. *Journal of Electron Spectroscopy and Related Phenomena*, **173**(1):7-11. [doi:10.1016/j.elspec.2009.03.001]
- Lin, S.S., Lu, J.G., Ye, Z.Z., He, H.P., Gu, X.Q., Chen, L.X., Huang, J.Y., Zhao, B.H., 2008. p-type behavior in Na-doped ZnO films and ZnO homojunction light-emitting diodes. *Solid State Communications*, **148**(1-2):25-28. [doi:10.1016/j.ssc.2008.07.028]
- Lin, S.S., He, H.P., Lu, Y.F., Ye, Z.Z., 2009. Mechanism of Na-doped p-type ZnO films: suppressing Na interstitials by codoping with H and Na of appropriate concentrations. *Journal of Applied Physics*, **106**(9):093508. [doi:10.1063/1.3254221]
- Liu, X.X., Lin, F.T., Sun, L.L., Cheng, W.J., Ma, X.M., Shi, W.Z., 2006. Doping concentration dependence of room-temperature ferromagnetism for Ni-doped ZnO thin films prepared by pulsed-laser deposition. *Applied Physics Letters*, **88**(6):062508. [doi:10.1063/1.2170420]
- Liu, E., Xiao, P., Chen, J. S., Lim, B. C., Li, L., 2008. Ni doped ZnO thin films for diluted magnetic semiconductor materials. *Current Applied Physics*, **8**(3-4):408-411. [doi:10.1016/j.cap.2007.10.025]
- Liu, X.J., Zhu, X.Y., Song, C., Zeng, F., Pan, F., 2009. Intrinsic and extrinsic origins of room temperature ferromagnetism in Ni-doped ZnO films. *Journal of Physics D: Applied Physics*, **42**(3):035004. [doi:10.1088/0022-3727/42/3/035004]
- Look, D.C., 2001. Recent advances in ZnO materials and devices. *Materials Science and Engineering B*, **80**(1-3):383-387. [doi:10.1016/S0921-5107(00)00604-8]
- McCluskey, M.D., Jokela, S.J., 2009. Defects in ZnO. *Journal of Applied Physics*, **106**(7):071101. [doi:10.1063/1.3216464]
- Mitra, S., Singh, S., Bandyopadhyay, S.K., Singh, C.S., 2006. Effect of irrigation, N, and bio-fertilizers on yield and nutrient uptake by wheat. *Tropical Agriculture*, **83**(1-4):87-94.
- Pan, F., Song, C., Liu, X.J., Yang, Y.C., Zeng, F., 2008. Ferromagnetism and possible application in spintronics of transition-metal-doped ZnO films. *Materials Science Engineering: R: Reports*, **62**(1):1-35. [doi:10.1016/j.mser.2008.04.002]
- Parra-Palomino, A., Perales-Perez, O., Singhal, R., Tomar, M., Hwang, J., Voyles, P.M., 2008. Structural, optical, and magnetic characterization of monodisperse Fe-doped ZnO nanocrystals. *Journal of Applied Physics*, **103**(7):07D121. [doi:10.1063/1.2834705]
- Peng, X.P., Zang, H., Wang, Z.G., Xu, J.Z., Wang, Y.Y., 2008. Blue-violet luminescence double peak of In-doped films prepared by radio frequency sputtering. *Journal of Luminescence*, **128**(3):328-332. [doi:10.1016/j.jlumin.2007.08.007]
- Sato, K., Katayama-Yoshida, H., 2001. Stabilization of ferromagnetic states by electron doping in Fe-, Co- or Ni-doped ZnO. *Japanese Journal of Applied Physics*, **40**:L334-L336. [doi:10.1143/JJAP.40.L334]
- Tang, Z.K., Wong, G.K.L., Yu, P., Kawasaki, M., Ohtomo, A., Koinuma, H., Segawa, Y., 1998. Room-temperature ultraviolet laser emission from self-assembled ZnO microcrystallite thin films. *Applied Physics Letters*, **72**(25):3270. [doi:10.1063/1.121620]
- Wagner, C.D., Riggs, W.M., Davis, L.E., Moulder, J.F., 1979. Handbook of X-ray Photoelectron Spectroscopy. Perkin Elmer, Eden Prairie, MN, USA, p.81.
- Wakano, T., Fujimura, N., Morinaga, Y., Abe, N., Ashida, A., Ito, T., 2001. Magnetic and magneto-transport properties of ZnO:Ni films. *Physica E: Low-Dimensional Systems and Nanostructures*, **10**(1-3):260-264. [doi:10.1016/S1386-9477(01)00095-9]
- Wang, Q., Sun, Q., Rao, B.K., Jena, P., 2004. Magnetism and energetics of Mn-Doped ZnO (10-10) thin films. *Physical Review B*, **69**(23):233310. [doi:10.1103/PhysRevB.69.233310]
- Yamada, T., Miyake, A., Kishimoto, S., Makino, H., Yamamoto, N., Yamamoto, T., 2007. Low resistivity Ga-doped ZnO thin films of less than 100 nm thickness prepared by ion plating with direct current arc discharge. *Applied Physics Letters*, **91**(5):051915. [doi:10.1063/1.2767213]
- Yu, G.H., Zeng, L.R., Zhu, F.W., Chai, C.L., Lai, W.Y., 2001. Magnetic properties and X-ray photoelectron spectroscopy study of NiO/NiFe films prepared by magnetron sputtering. *Journal of Applied Physics*, **90**(8):4039. [doi:10.1063/1.1401804]
- Yu, W., Yang, L.H., Teng, X.Y., Zhang, J.C., Zhang, Z.C., Zhang, L., Fu, G.S., 2008. Influence of structure characteristics on room temperature ferromagnetism of Ni-doped ZnO thin films. *Journal of Applied Physics*, **103**(9):093901. [doi:10.1063/1.2903524]
- Zeng, Y.J., Ye, Z.Z., Lu, J.G., Xu, W.Z., Zhu, L.P., Zhao, B.H., Limpijumnong, S., 2006. Identification of acceptor states in Li-doped p-type ZnO thin films. *Applied Physics Letters*, **89**(4):042106. [doi:10.1063/1.2236225]